

# Conformational Transitions in Adenylate Kinase

## ALLOSTERIC COMMUNICATION REDUCES MISLIGATION\*

Received for publication, September 11, 2007, and in revised form, October 26, 2007. Published, JBC Papers in Press, November 11, 2007, DOI 10.1074/jbc.M707632200

Paul C. Whitford<sup>1</sup>, Shachi Gosavi<sup>2</sup>, and José N. Onuchic<sup>3</sup>

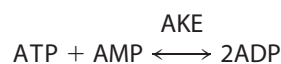
From the Center for Theoretical Biological Physics and the Department of Physics, University of California at San Diego, La Jolla, California 92093

Large conformational changes in the LID and NMP domains of adenylate kinase (AKE) are known to be key to ligand binding and catalysis, yet the order of binding events and domain motion is not well understood. Combining the multiple available structures for AKE with the energy landscape theory for protein folding, a theoretical model was developed for allostery, order of binding events, and efficient catalysis. Coarse-grained models and nonlinear normal mode analysis were used to infer that intrinsic structural fluctuations dominate LID motion, whereas ligand-protein interactions and cracking (local unfolding) are more important during NMP motion. In addition, LID-NMP domain interactions are indispensable for efficient catalysis. LID domain motion precedes NMP domain motion, during both opening and closing. These findings provide a mechanistic explanation for the observed 1:1:1 correspondence between LID domain closure, NMP domain closure, and substrate turnover. This catalytic cycle has likely evolved to reduce misligation, and thus inhibition, of AKE. The separation of allosteric motion into intrinsic structural fluctuations and ligand-induced contributions can be generalized to further our understanding of allosteric transitions in other proteins.

Kinase-mediated phosphoryl transfer is a key component of many signaling pathways. Tight control of signaling requires regulation of kinase activity, which is influenced by allosteric transitions (1, 2). The classical description of allostery involves ligand-induced conformational rearrangements between static protein structures. It is now acknowledged that protein dynamics is statistical in nature and that allostery is often due to a change in the balance of pre-existing conformational substates upon ligand binding (3).

This manuscript explores the subject of how protein structure determines allostery, order of ligand binding events, and ultimately, efficient catalysis, in the context of adenylate kinase

(AKE).<sup>4</sup> AKE is a three-domain (LID, NMP, and CORE) protein (Fig. 1) that undergoes large conformational changes as it catalyzes Reaction 1.



REACTION 1

Large motions of the LID and NMP domains are associated with nucleotide binding. It has been shown that substrate turnover and domain rearrangements (“open” state to “closed” state) occur at the same frequency (2). Despite several theoretical (6–13) and experimental studies (2, 14–17) on AKE, a catalytic mechanism that explains this high efficiency has not been proposed.

Because it is known that conformational transitions can be well described as a superposition of normal modes (6, 7, 13, 18–20), we use a simplified nonlinear elastic network model and a structure-based model with implicit ligand interactions to demonstrate a likely catalytic mechanism in AKE. We show that intrinsic structural fluctuations (21, 22) in the LID domain account for the majority of the domain’s motion and that ATP binding likely serves to lock the domain closed. The LID motion is an example of allosteric regulation that results from a shift in the populations of available substates. The intrinsic motion of the NMP domain does not correlate with domain closure. Thus, the NMP domain is an example of a ligand-induced conformational change. Additionally, the high strain in the NMP domain supports the claim that the NMP domain likely partially unfolds (cracks) during conformational transitions. Upon closure of the LID domain, the LID-NMP interface provides enthalpic interactions that stabilize the closed NMP domain. This provides a driving force for NMP closure and leads to phosphoryl transfer. Intrinsic structural fluctuations then drive the LID domain open, which destabilizes the LID-NMP interface and drives the NMP domain open. This mechanism, which involves correlated motion of the domains, reduces misligation and may have evolved to increase the efficiency of AKE.

## MATERIALS AND METHODS

*Multiple Minima Molecular Dynamics Simulations*—Structure-based models allow one to study the relationship between protein folding (24–29) and protein function (8, 30–32). To characterize the energetics of the conformational change tran-

\* This work was supported in part by Grants PHY-0216576 and 0225630 from the National Science Foundation (NSF)-sponsored Center for Theoretical Biological Physics and NSF Grant 0543906. The costs of publication of this article were defrayed in part by the payment of page charges. This article must therefore be hereby marked “advertisement” in accordance with 18 U.S.C. Section 1734 solely to indicate this fact.

<sup>1</sup> Supported by National Institutes of Health Molecular Biophysics Training Program at University of California at San Diego Grant T32 GM08326.

<sup>2</sup> Supported in part by a Burroughs Wellcome Fund La Jolla Interfaces in Science fellowship.

<sup>3</sup> To whom correspondence should be addressed: Center for Theoretical Biological Physics, University of California at San Diego, 9500 Gilman Dr., La Jolla, CA 92093. Fax: 858-534-7697; E-mail: jonuchic@ucsd.edu.

<sup>4</sup> The abbreviations used are: AKE, adenylate kinase; NMA, normal mode analysis; MD, molecular dynamics; PDB, Protein Data Bank; CM, center of mass.

sition states of AKE, we simulated it using a coarse-grained, structure-based potential that utilizes information from the open and closed forms. Each residue was represented by a bead located at the  $C_{\alpha}$  position. Backbone geometry was maintained through harmonic potentials for adjacent bond distances and bond angles and through cosine functions for dihedrals, with minimum values corresponding to the open conformation (PDB code 4AKE (4)). Non-local contacts were determined using contact of structural units analysis (33) of the open conformation and are included via a 10–12 potential. Non-contacts were given repulsive terms. In addition to the open contacts, contacts unique to the closed structure (PDB code 1AKE (5)) were included to induce domain closure. The closed contacts provide an implicit representation of the ligand. A complete description of the potential can be found elsewhere (8). For this study, we reduced the interaction strength of all contacts formed with helix 4 $\alpha$  by 30%. Reducing these interaction strengths noticeably alters the population of the NMP-closed-LID-open conformation, which illustrates the significant effect helix 4 $\alpha$  has on the catalytic dynamics.

**Nonlinear Normal Mode Analysis**—Normal modes are known to capture the dynamics of large conformational changes in many proteins (6, 7, 23). In this study we used a nonlinear normal mode analysis to describe the intrinsic contributions a given structure provides to each conformational rearrangement. This approach, first introduced by Miyashita *et al.* (6, 7), provides a better representation of global motion far from equilibrium by minimizing steric and energetic contradictions observed by standard linear normal mode analysis.

Initially, normal modes  $\tilde{N}_i$  for the open form of AKE (PDB code 4AKE) were determined using a Tirion potential (34), where all atom pairs within 5 Å are connected by harmonic springs. AKE was translated along each mode a distance of  $dR_i = \Lambda \tilde{d} \cdot \tilde{N}_i B_i / B_t$ , where  $B_i / B_t$  is the fraction of the total B-factor contributed by mode  $i$  and  $\Lambda$  is a chosen length scale (=0.05 Å).  $\tilde{d}$  is the spatial displacement of atoms between the current structure and the final structure (closed structure, PDB code 1AKE) after root mean squared fitting using the McLachlan algorithm (35) in the ProFit software package (because  $\tilde{d}$  and root mean squared fitting require two structures with an identical number of atoms and the open structure does not have a ligand, ligands were not explicitly represented). Thus, the intrinsic overlap with a conformational change is as follows.

$$\frac{1}{\Lambda} \sum_i^{\text{modes}} dR_i$$

At every step, a new Tirion potential was determined based on the translated structure, and the nonlinear normal mode analysis was repeated. This process was repeated until the closed conformation was reached. The same process was used for the opening of AKE and for individual domain rearrangements. This method is similar to a previously applied method (5, 6), except that the  $B_i / B_t$  term in  $dR_i$  was not included in previous studies. Although the  $B_i / B_t$  term does not qualitatively alter the dynamics, it modifies overlap to be the percent of intrinsic motion a structure has in the direction of a given conforma-

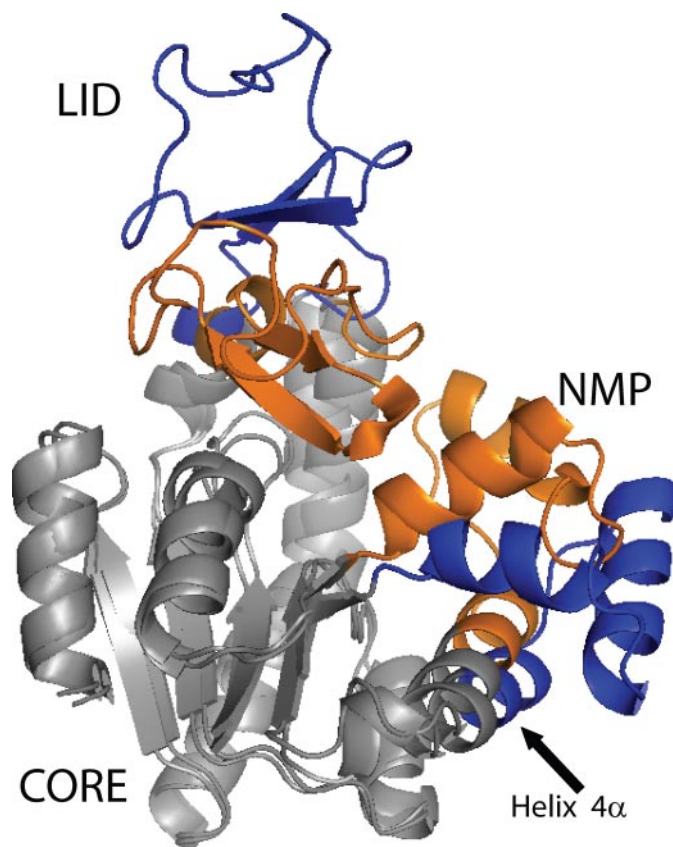


**FIGURE 1. Crystal structures of AKE.** Shown are the structures of the open (blue, PDB code 4AKE (4)) and closed (orange, PDB code 1AKE (5)) LID and NMP domains of AKE, with the CORE domain (gray) spatially aligned. AKE can accommodate two ligands, one in the pocket between the LID and CORE domains and one in the NMP-CORE pocket. ATP, ADP, and AMP are able to bind to the LID-CORE pocket. ADP and AMP are able to bind to the NMP-CORE pocket.

tional transition. The strain energy was determined by calculating the total potential energy as defined by the Tirion potential for the initial structure. As discussed by Miyashita *et al.* (6, 7), if too much local strain is accumulated then cracking (local unfolding) may reduce the strain during conformational transitions.

**Reaction Coordinates**—Allosteric conformational changes involve major domain motion. We measured this motion using the spatial distance between the center of masses of the domains.  $R_{CM}^{LID-CORE}$  and  $R_{CM}^{NMP-CORE}$  are the distances between the center of mass of the LID and the CORE domains and the distance between the center of mass of the NMP and the CORE domains, respectively.  $R_{CM}^{LID-CORE}$  is 30.1 and 21.0 Å in the open and closed forms, respectively, whereas  $R_{CM}^{NMP-CORE}$  is 22.0 and 18.4 Å in the open and closed forms, respectively. The LID domain is defined as residues 118–160, the NMP domain as residues 30–67, and the CORE domain as residues 1–29, 68–117, and 161–214.

## RESULTS

**Intrinsic Motion in the LID Domain of AKE Contributes Significantly to Allosteric Motion**—The LID and NMP domains of AKE rearrange relative to the CORE domain during catalysis (Fig. 1). To determine the order of domain motion, closing and

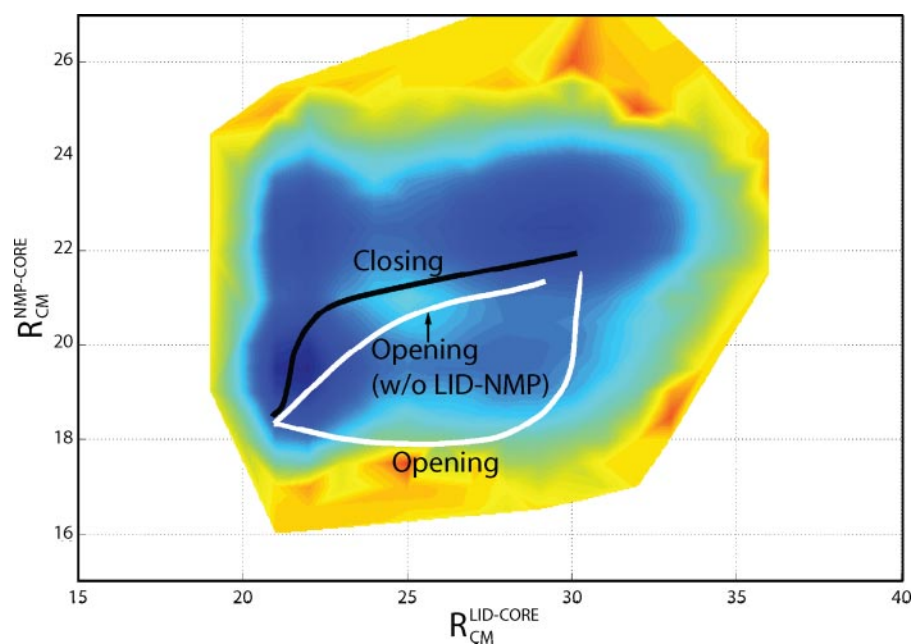


**FIGURE 2. Intrinsic fluctuations direct conformational dynamics.** Nonlinear normal mode trajectories are superimposed on the free energy landscape obtained via MD simulations. Axes are the distance between the LID domain and CORE domain centers of mass,  $R_{CM}^{LID-CORE}$ , and the distance between the NMP domain and CORE domain centers of mass,  $R_{CM}^{NMP-CORE}$ . NMA suggests sequential closing and opening of the LID and NMP domains in agreement with the free energy landscape. Intrinsic fluctuations promote LID opening prior to NMP opening. Removal of LID-NMP interactions eliminates the NMP domain's dependence on the LID domain during opening. The normal mode trajectories begin and end at the crystal structures of AKE. The free energy minima for the open and closed forms are at slightly larger values of  $R_{CM}^{LID-CORE}$  and  $R_{CM}^{NMP-CORE}$  because of higher entropy in more extended structures. When normal mode trajectories are shifted to slightly larger  $R_{CM}$  values, there is excellent agreement between the two methods.

opening trajectories were constructed using recursive nonlinear normal mode analysis (see "Materials and Methods"). At every step of this recursive procedure, the domains were translated along each mode by an amount proportional to the mode's overlap with the conformational transition. This process filters for high B-factor-contributing and high conformational overlap modes. Because B-factors are a measure of atom mobility within a protein, this method not only determines a likely pathway but also provides a quantitative measure for the intrinsic (ligand-free) propensity of the protein to undergo a given conformational rearrangement.

Fig. 2 shows the trajectories as functions of  $R_{CM}^{LID-CORE}$  and  $R_{CM}^{NMP-CORE}$ , the distances between the center of masses of the LID and CORE domains and of the NMP and CORE domains. These trajectories indicate that LID domain motion precedes NMP domain motion during both the opening and closing processes. There are two possible explanations for this observed sequential motion. 1) The open (closed) protein has the intrinsic ability to close (open) the LID domain and not the NMP domain. Once the LID domain closes (opens), the dynamics of the NMP domain are altered such that the intrinsic fluctuations in the LID-closed (open) state favor NMP closure (opening). 2) There is an intrinsic ability to close (open) the LID domain and not the NMP domain. After LID closure (opening), the method employed merely forces the NMP domain to close (open).

*The LID-NMP Interface Facilitates Communication between LID and NMP*—To determine the reason for the observed sequential motion, trajectories were constructed for individual domain rearrangements (Fig. 3). LID domain motion has a

higher intrinsic overlap and lower strain associated with its motion than does NMP motion. When both domains are open or closed, there are lower barriers associated with LID motion than NMP motion. Also, a significant increase (Fig. 3,  $\star$  versus  $\star\star$ ) in the slope of the strain associated with NMP opening is observed upon the LID-NMP interface formation.

The combination of a reduced intrinsic overlap and the higher energetic barriers associated with NMP motion suggests that NMP motion is more dependent on enthalpic contributions, such as ligand binding and LID-NMP interface formation. Additionally, the low intrinsic overlap suggests the NMP domain may enter a disordered (locally unfolded) state during conformational transitions. This agrees with structure-based simulations of the open form of AKE that have shown the closed LID domain is more easily accessible than the closed NMP state (see Fig. 4a of Ref. 8) and that local unfolding is

observed in the NMP domain (see Fig. 5 of Ref. 8). Additionally, because the LID domain has a propensity to close and the NMP domain does not, stabilizing interactions must be available to close the NMP domain.

*LID Domain Binding of ATP Assists NMP Closure*—Using a simplified structure-based potential (see "Materials and Methods") and MD simulations, the free energy surface of the conformational rearrangements in AKE was calculated (Fig. 2).<sup>5</sup> This model suggests strong coupling between NMP and LID motion in agreement with the nonlinear normal mode trajectories. Using the transition state ensembles for each domain's motion, we can calculate functional Phi values  $\Phi_{Func}$ , which are analogous to protein-folding  $\Phi$  values. Protein-folding  $\Phi$  values measure the free energy contribution to the folding transition state relative to the native state (36) for a given residue. Because proteins tend to be minimally frustrated, folding results from the balance between the entropy of the unfolded state and native enthalpic interactions. Thus,  $\Phi$  values measure the amount a given residue drives the folding process. Because the entropy of the various conformations of an allosteric protein may be comparable, enthalpic contributions may play a large role in both the forward and reverse conformational transitions. Thus, high  $\Phi_{Func}$  values show a given transition is dominated by enthalpic interactions, and low  $\Phi_{Func}$  values show intrinsic structural fluctuations dominate the transition.

<sup>5</sup> A discrepancy exists between the normal mode trajectories and the locations of the free energy minima because the MD landscape includes entropic contributions.

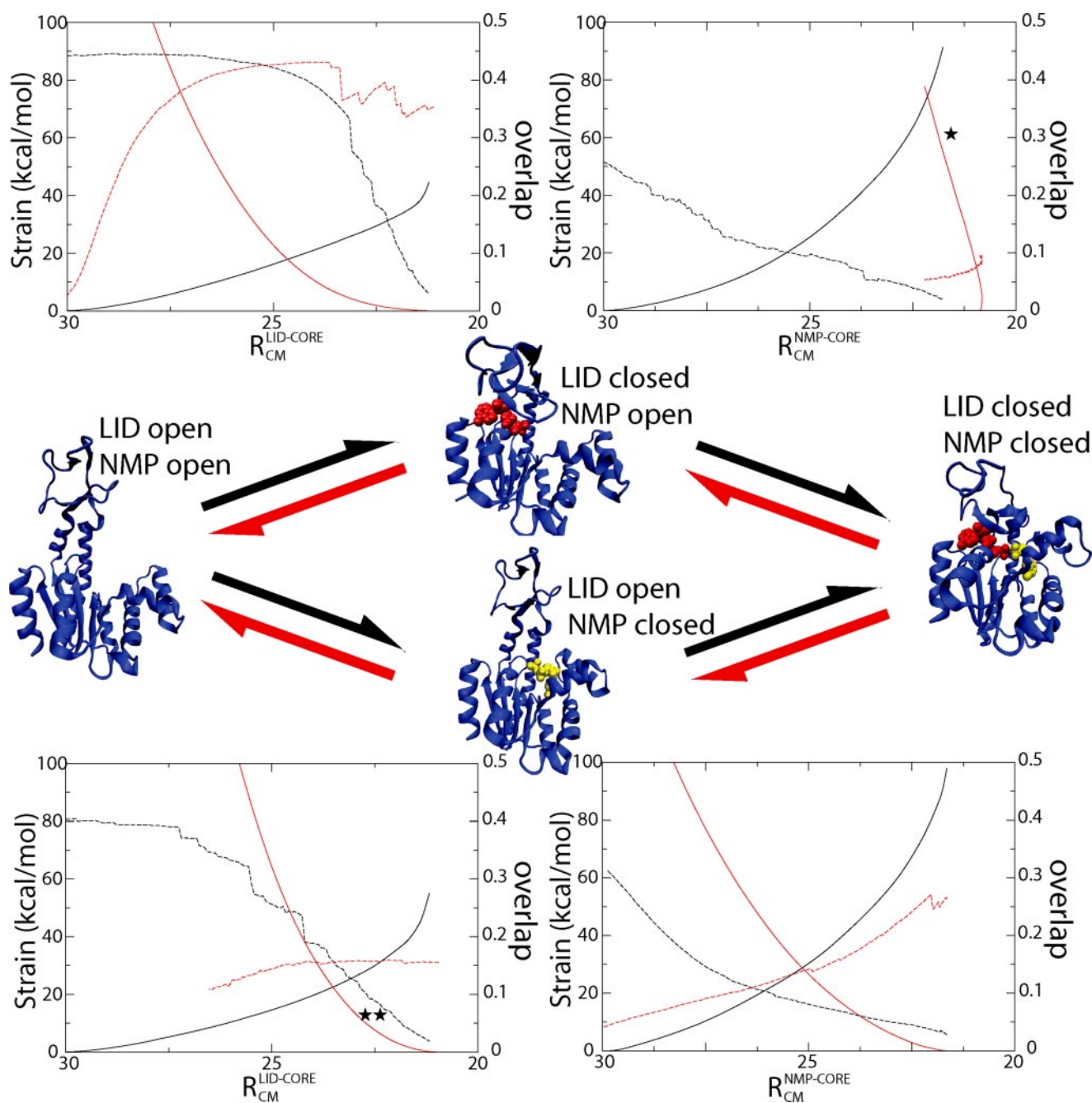


**FIGURE 3. Intrinsic motion of LID domain overlaps with allosteric conformational transition.** Four possible conformations during catalysis are shown with the associated overlap and energetic barriers: both domains open, the LID domain closed with the NMP domain open, both domains closed, and the LID domain open with the NMP domain closed. *Solid lines* correspond to the strain associated with opening (*black*) and closing (*red*) each domain. *Dotted lines* represent the intrinsic overlap of opening (*black*) and closing (*red*). LID domain closure has a higher intrinsic overlap ( $\approx 0.45$ ) than does NMP domain closure ( $\approx 0.4$ ), and the NMP overlap drops more quickly as the domain closes (decreasing  $R_{CM}$ ). Thus, it is likely that the interactions that stabilize the closed state are more important for NMP closure than for LID closure. The largest energetic barrier is associated with NMP opening prior to LID opening. The barrier associated with NMP motion when the LID domain is closed (\*) is greater than when the LID domain is open (\*\*). This larger barrier height is due to the steep strain profile associated with opening of the NMP domain. Because the most significant structural difference involving the NMP domain is the degree of LID-NMP interface formation, this interface probably plays a role in regulating domain motion, and ultimately activity. The third important feature is the higher intrinsic overlap with LID opening ( $\approx 0.3$ ) than with NMP opening ( $\approx 0.1$ ). The fourth feature is that the overlap of NMP opening increases by 50% when the LID domain is already open. These last two features further illustrate the significant effect the LID-NMP interface has on catalytic dynamics.

Therefore, one can determine whether a given residue with a high  $\Phi_{Func}$  stabilizes the forward or the backward reaction.

Larger  $\Phi_{Func}$  values for the NMP domain suggest that energetics is more important for NMP motion than for LID motion.  $\Phi_{Func}$  values for residues at the LID-NMP interface are large for the NMP transition state but nearly zero for the LID transition

state. Therefore, not only is NMP motion highly dependent on enthalpic interactions, but also a significant number of these interactions are made accessible through closure of the LID domain. This suggests that NMP motion is strongly influenced by the state of the LID domain (open/closed) as well as by AMP binding to its binding site. Thus, both nonlinear normal mode

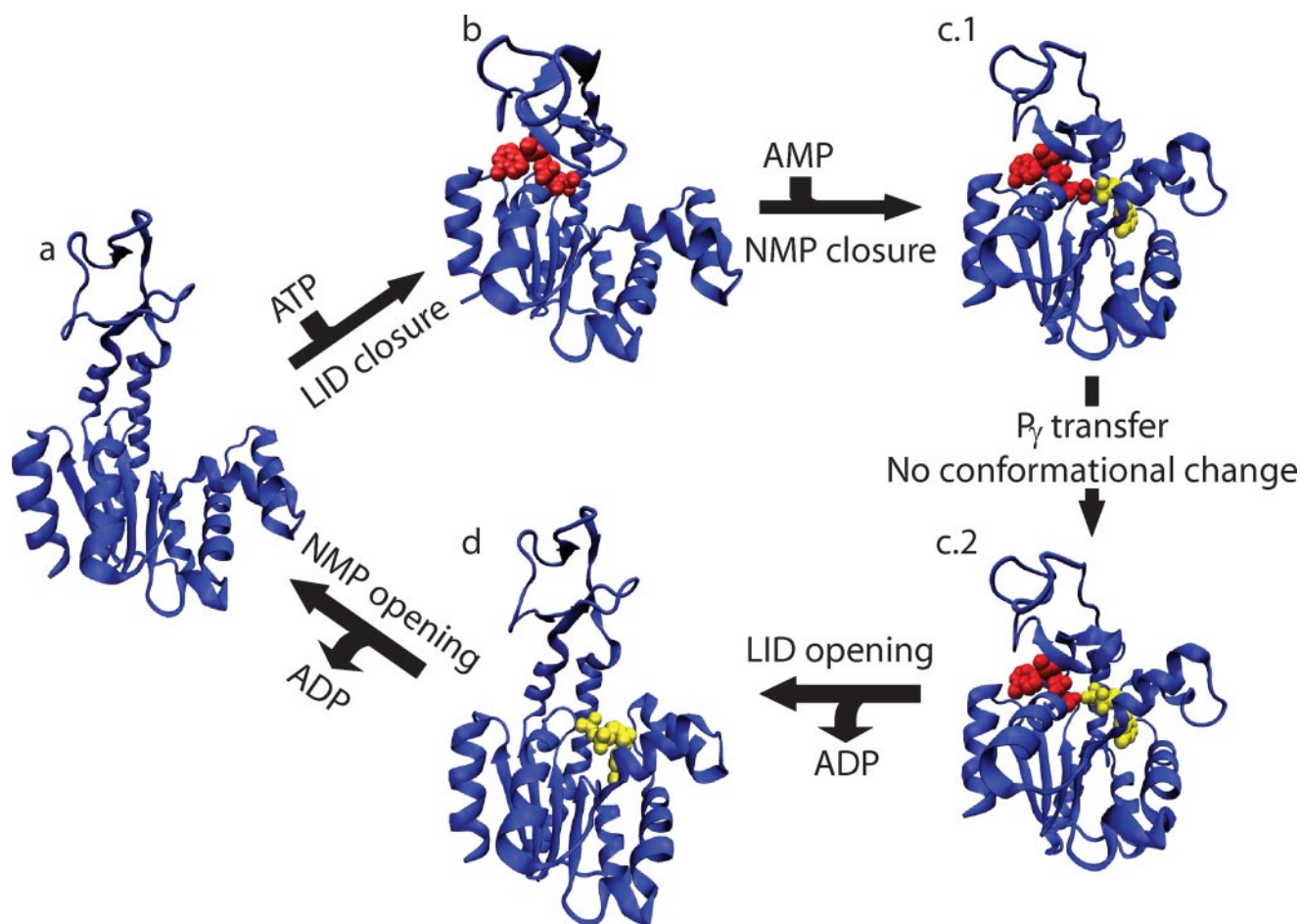


FIGURE 4. **Proposed mechanism for AKE catalysis.** All results presented suggest the following catalytic mechanism for AKE. *a*, open, unligated AKE. *b*, ATP binds while the LID domain closes. *c.1*, closure is followed by AMP binding/NMP domain closure. *c.2*, phosphoryl transfer occurs, resulting in two bound ADPs. *d*, thermal fluctuations open LID domain and one ADP is released. *a*, the loss of LID-CORE interactions induces opening of NMP domain, loss of the second ADP, and a return to the open conformation. States *c.1* and *c.2* are modeled by the deletion of one phosphoryl group from Ap5A in PDB code 1AKE.

analysis and MD simulations suggest that intrinsic fluctuations are not the main contributors to the NMP transition.

*Domain Dynamics Can Be Controlled by Mutating the LID-NMP Interface and Helix 4 $\alpha$* —To test the importance of the LID-NMP interface on NMP domain dynamics, nonlinear normal mode analysis (NMA) was performed with all LID-NMP interface interactions removed (Fig. 2). As expected, the LID domain no longer opens prior to NMP opening.<sup>6</sup> Additionally, if the LID-NMP interactions are not included in our MD simulations, the population of the NMP closed state is largely reduced. Because the interface plays a large role in stabilizing the closed NMP domain and the entropy of the open and closed states is approximately the same (data not shown), enthalpic contributions must stabilize the open form. Helix 4 $\alpha$  in the NMP domain fulfills this role. We repeated our previous simulations (8) using varying interaction strengths for native contacts made with helix 4 $\alpha$  (Fig. 2). By reducing the strength of these interactions in simulations we are able to alter the domain dynamics such that NMP closure followed by LID closure was as probable as LID closure followed by NMP closure. Additionally, by removing the LID-NMP interactions in our NMA we

<sup>6</sup> The closing trajectories were not repeated without LID-NMP interactions, as these interactions are not formed in the open conformation.

changed the opening dynamics such that NMP opening precedes LID opening (Fig. 2). These results illustrate the dramatic effects that the LID-NMP interface and helix 4 $\alpha$  have on the catalytic dynamics of AKE.

## DISCUSSION

*Catalytic Cycle Explains the 1:1:1 Relationship among NMP Motion, LID Motion, and Substrate Turnover*—Although the NMP and the LID domains are allowed to move independently (37, 38), their conformational transition rates are equal (2). Despite evidence that substrate turnover and domain motion are correlated, the details of the mechanism are still unknown. The data presented in this manuscript suggest a catalytic cycle in which there is time-ordered and sequential domain motion (Fig. 4), *i.e.* LID domain motion precedes NMP motion. Assuming fast phosphoryl transfer, independent domain motion, correct ligand binding, and conformational exchange rates of  $k_{\text{LID}}$  and  $k_{\text{NMP}}$ , the substrate turnover rate would be  $k_{\text{P}} = 2/((1/k_{\text{LID}}) + (1/k_{\text{NMP}}))$ . This rate is less than  $k_{\text{LID}}$  and  $k_{\text{NMP}}$  unless  $k_{\text{LID}} = k_{\text{NMP}}$ . Having independent domain motion that coincidentally has the exact same exchange rate is unlikely. Thus, an alternate explanation for  $k_{\text{P}} = k_{\text{LID}} = k_{\text{NMP}}$  is that domain rearrangement is correlated, where the closure (opening) of one

domain signals the rapid closure (opening) of the second domain. Energetic and structural considerations from simplified simulations and nonlinear normal mode analysis suggest LID motion signals NMP motion in the following catalytic mechanism. 1) AKE is in the unligated open conformation (Fig. 4*a*). 2) The LID domain closes and ATP binds (Fig. 4*b*). 3) LID closure enables AMP to bind concomitantly with NMP domain closure (Fig. 4*c.1*). 4) Phosphoryl transfer occurs, resulting in two bound ADPs (Fig. 4*c.2*). 5) ADP is released from the ATP site and the LID domain opens (Fig. 4*d*). 6) Opening of the LID domain signals the NMP domain to open and release the second ADP (Fig. 4*a*).

**Catalytic Cycle Prevents Misligation**—The proposed closing mechanism ensures that each conformational rearrangement contributes to the turnover of a substrate by preventing nonproductive substrate binding. Several structural features of AKE are consistent with the proposed mechanism. 1) The  $\text{LID}_{\text{ATP}}^{\text{C}}\text{-NMP}_{\text{AMP}}^{\text{C}}$  complex is the only product-forming state.<sup>7</sup> 2) The ATP binding site (LID-CORE pocket) can accommodate ATP, ADP, and AMP (in order of decreasing affinity). 3) The AMP binding site (NMP-CORE pocket) is only known to accommodate ADP and AMP.<sup>8</sup> 4) When in the  $\text{LID}_{\text{ATP}}^{\text{C}}\text{-NMP}_0^{\text{O}}$  state, the AMP site can only accommodate AMP.

During step 1, the binding affinities at the ATP site discriminate ATP over AMP by 3 kcal/mol (17). Because the  $\text{LID}_{\text{ATP}}^{\text{C}}\text{-NMP}_0^{\text{O}}$  state can only accommodate an AMP,<sup>9</sup> proper ligation in AKE would be limited by the ability of the ATP site to discriminate between AMP and ATP. If the alternate closing mechanism was common ( $\text{LID}_0^{\text{O}}\text{-NMP}_{\text{AMP}}^{\text{C}}$  followed by  $\text{LID}_{\text{ATP}}^{\text{C}}\text{-NMP}_{\text{AMP}}^{\text{C}}$ ), AKE would have more opportunities to form non-product-forming (inhibited) complexes. In the  $\text{LID}_0^{\text{O}}\text{-NMP}_{\text{AMP}}^{\text{C}}$  state the NMP domain is closed. NMP domain closure grants the LID domain access to the LID-NMP interface interactions. These interactions could reduce discrimination between the  $\text{LID}_{\text{ATP}}^{\text{C}}\text{-NMP}_{\text{AMP}}^{\text{C}}$  and  $\text{LID}_{\text{AMP}}^{\text{C}}\text{-NMP}_{\text{AMP}}^{\text{C}}$  states by perturbing the closing dynamics of the LID domain. In addition, the LID-NMP interface may provide enough stability to the closed LID domain so that the LID may temporarily close without a ligand. If an ATP-free, LID-closed state is formed, the LID domain would have to open prior to substrate binding and turnover. Thus, these nonfunctional states would increase domain motion frequency without yielding product.

Similar structural/functional arguments support the proposed opening process (steps 5 and 6). In Fig. 4, the LID-bound ADP is released first (LID opening), resulting in the  $\text{LID}_0^{\text{O}}\text{-NMP}_{\text{ADP}}^{\text{C}}$  state. Upon LID opening the interface between the NMP domain and the LID domain is lost, which destabilizes the closed NMP state. In addition to this destabilization, the intrinsic fluctuations of NMP increase in the direction of domain

opening (Fig. 3). The combination of NMP domain destabilization, increased motion in the opening direction, and the chemical potential driving ADP out of the NMP-CORE pocket likely signal the NMP domain to open. These contributions ensure rapid release of the second ADP, allowing NMP to open without the  $\text{LID}_{\text{AMP}}^{\text{C}}\text{-NMP}_{\text{ADP}}^{\text{C}}$  state forming.

Strain energy considerations from molecular dynamics simulations (8) and NMA suggest the alternate opening mechanism, namely NMP opening followed by LID opening, would also be more error prone. To see why, consider the two closed domains to be loaded springs that have been pulled from their equilibrium (open) states. MD simulations and NMA suggest there is a larger amount of strain buildup during NMP closure than during LID closure (approximately three times more; see Fig. 3 and Ref. 8). Assuming one of the domains is open and the other is closed, the smaller mass of the NMP domain and larger effective spring constant ( $\propto$  strain) make it open approximately twice as fast as the LID domain. Thus, when the NMP domain opens first there is twice as much time available for AKE to misligate (forming a  $\text{LID}_{\text{ATP}}^{\text{C}}\text{-NMP}_{\text{ADP}}^{\text{C}}$  complex) than if the LID opens first (forming a  $\text{LID}_{\text{ADP}}^{\text{C}}\text{-NMP}_{\text{AMP}}^{\text{C}}$  complex).

**Predictions for the AKE Catalytic Cycle**—As described above, helix 4 $\alpha$  and LID-NMP interface appear to play large roles in the catalytic activity of AKE. To probe these effects in experiments, activity assays of different mutants can be performed. Mutations that provide strong interactions between helix 4 $\alpha$  and nearby residues may either maintain wild-type efficiency (substrate turnover/domain rearrangement  $\approx$  1) or result in NMP domain motion becoming extremely rate-limiting. In the latter case, the NMP domain will undergo a single transition per substrate turnover, even though the LID domain undergoes many closing/opening transitions.

On the other hand, mutations that destabilize helix 4 $\alpha$  and the LID-NMP interface would allow NMP to close more easily, diminish the role of the LID-NMP interface, and decouple the motion of the two domains. This decoupling would effectively poison the protein and substrate turnover would drop to  $2/((1/k_{\text{LID}}) + (1/k_{\text{NMP}}))$ , assuming no misligation events.

**Allosteric Motion May Be Decomposed into Intrinsic and Ligand-gated Contributions**—Allosteric conformational transitions are becoming a prevalent theme in cellular signaling, occurring in a wide range of systems, including kinases, G-proteins, and ion channels. In the classical view of allostery, conformational changes occur between static structures and are induced by ligand binding. Allosteric changes of this type can be considered “ligand-gated” or “extrinsic” motion. In contrast, the current understanding of allostery assumes that protein structures are not static, three-dimensional structures but are ensembles of conformations where ligands change the balance of pre-existing substates. In this perspective, the protein is constantly interconverting between multiple conformations, and the conformational change could be considered “intrinsic.” In this manuscript we have included the intrinsic and extrinsic descriptions in a single statistical picture and provided two structure-based methods that quantitatively distinguish between them. Using AKE as a test protein, we have demonstrated that the conformational rearrangement of the LID

<sup>7</sup> The following notations were used:  $\text{LID}_Y^X$  = LID domain in state X (O = open, C = closed) with Y (ATP, ADP, AMP, or 0 = no ligand) bound to the LID-CORE pocket; and  $\text{NMP}_Y^X$  = NMP domain in state X (O = open, C = closed) with Y (ATP, ADP, AMP) bound to the NMP-CORE pocket.

<sup>8</sup> Because of communication between domains and AMP binding of the ATP site, binding affinities for AMP may be difficult to determine exactly.

<sup>9</sup> Because Reaction 1 is reversible,  $\text{LID}_{\text{ADP}}^{\text{C}}\text{-NMP}_{\text{ADP}}^{\text{C}}$  can result in a product, although in this manuscript we assume steady-state conditions for the forward reaction.

## Conformational Transitions in Adenylate Kinase

domain can be captured by intrinsic motion and that the motion of the NMP domain is likely more dependent on ligands. As we target allosteric changes in therapeutics, this type of classification will allow for more sophisticated drug design.<sup>9</sup>

*Acknowledgments*—We thank Professor Peter Wolynes and Jeffrey Noel for valuable discussions, especially regarding NMA, and Patricia Jennings for discussion about enzymatic kinetics.

### REFERENCES

1. Lieser, S. A., Shaffer, J., and Adams, J. A. (2007) *J. Biol. Chem.* **281**, 38004–38012
2. Wolf-Watz, M., Thai, V., Henzler-Wildman, K., Hadjipavou, G., Eisenmesser, E. Z., and Kern, D. (2004) *Nat. Struct. Biol.* **11**, 945–949
3. Eisenmesser, E., Millet, O., Labeikovsky, W., Korzhnev, D. M., Wolf-Watz, M., Bosco, D. A., Skalicky, J. J., Kay, L. E., and Kern, D. (2005) *Nature* **438**, 117–121
4. Mueller, C. W., Schlauderer, G. J., Reinstein, J., and Schulz, G. E. (1996) *Structure (Camb.)* **4**, 147–156
5. Mueller, C. W., and Schulz, G. E. (1992) *J. Mol. Biol.* **224**, 159–177
6. Miyashita, O., Onuchic, J. N., and Wolynes, P. G. (2003) *Proc. Natl. Acad. Sci. U. S. A.* **100**, 12570–12575
7. Miyashita, O., Wolynes, P. G., and Onuchic, J. N. (2005) *J. Phys. Chem. B* **109**, 1959–1969
8. Whitford, P. C., Miyashita, O., Levy, Y., and Onuchic, J. N. (2007) *J. Mol. Biol.* **366**, 1661–1671
9. Krishnamurthy, H., Lou, H., Kimple, A., Vieille, C., and Cukier, R. (2005) *Proteins Struct. Funct. Bioinform.* **58**, 88–100
10. Lou, H., and Cukier, R. I. (2006) *J. Phys. Chem. B* **110**, 24121–24137
11. Snow, C., Qi, G., and Hayward, S. (2007) *Proteins Struct. Funct. Bioinform.* **67**, 325–337
12. Temiz, N. A., Meirovitch, E., and Bahar, I. (2004) *Proteins Struct. Funct. Bioinform.* **57**, 468–480
13. Maragakis, P., and Karplus, M. (2005) *J. Mol. Biol.* **352**, 807–822
14. Bae, E., and Phillips, G. N. (2004) *J. Biol. Chem.* **279**, 28202–28208
15. Bae, E., and Phillips, G. N. (2006) *Proc. Natl. Acad. Sci. U. S. A.* **103**, 2132–2137
16. Sinev, M. A., Sineva, E. V., Ittah, V., and Haas, E. (1996) *Biochemistry* **35**, 6425–6437
17. Sanders, C. R., Tian, G., and Tsai, M. D. (1989) *Biochemistry* **28**, 9028–9043
18. Moritsugu, K., and Kidera, A. (2004) *J. Phys. Chem. B* **108**, 3890–3898
19. Horiuchi, T., and Gō, N. (1991) *Proteins Struct. Funct. Genet.* **10**, 106–116
20. Kong, Y., Ma, J., Karplus, M., and Lipscomb, W. (2006) *J. Mol. Biol.* **356**, 237–247
21. Gerstein, M., Lesk, A. M., and Chothia, C. (1994) *Biochemistry* **33**, 6739–6749
22. Bahar, I., Atilgan, A. R., and Erman, B. (1997) *Folding Des.* **2**, 173–181
23. Tama, F., and Sanejouand, Y. H. (2001) *Protein Eng.* **14**, 1–6
24. Bryngelson, J. D., Onuchic, J. N., Socci, N. D., and Wolynes, P. G. (1995) *Proteins* **21**, 167–195
25. Bryngelson, J. D., and Wolynes, P. G. (1987) *Proc. Natl. Acad. Sci. U. S. A.* **84**, 7524–7528
26. Leopold, P. E., Montal, M., and Onuchic, J. N. (1992) *Proc. Natl. Acad. Sci. U. S. A.* **18**, 8721–8725
27. Onuchic, J. N., and Wolynes, P. G. (2004) *Curr. Opin. Struct. Biol.* **14**, 70–75
28. Clementi, C., Nymeyer, H., and Onuchic, J. N. (2000) *J. Mol. Biol.* **298**, 937–953
29. Nymeyer, H., Garcia, A. E., and Onuchic, J. N. (1998) *Proc. Natl. Acad. Sci. U. S. A.* **95**, 5921–5928
30. Levy, Y., Cho, S. S., Shen, T., Onuchic, J. N., and Wolynes, P. G. (2005) *Proc. Natl. Acad. Sci. U. S. A.* **102**, 2373–2378
31. Levy, Y., Cho, S. S., Onuchic, J. N., and Wolynes, P. G. (2005) *J. Mol. Biol.* **346**, 1121–1145
32. Yang, S. C., Cho, S. S., Levy, Y., Cheung, M. S., Levine, H., Wolynes, P. G., and Onuchic, J. N. (2004) *Proc. Natl. Acad. Sci. U. S. A.* **101**, 13786–13791
33. Sobolev, V., Wade, R., Vried, G., and Edelman, M. (1996) *Proteins Struct. Funct. Genet.* **25**, 120–129
34. Tirion, M. M. (1996) *Phys. Rev. Lett.* **77**, 1905–1908
35. McLachlan, A. D. (1982) *Acta Crystallogr. Sect. A* **38**, 871–873
36. Fersht, A. (1994) *Curr. Opin. Struct. Biol.* **4**, 79–84
37. Schlauderer, G. J., Proba, K., and Schulz, G. E. (1996) *J. Mol. Biol.* **256**, 223–227
38. Diederichs, K., and Schulz, G. E. (1991) *J. Mol. Biol.* **217**, 541–549